PHYSICAL REVIEW MATERIALS **1**, 014401 (2017)

Dynamical multiferroicity

Dominik M. Juraschek,[1,*] Michael Fechner,[1,2] Alexander V. Balatsky,[3,4,5] and Nicola A. Spaldin[1]

[1]*Materials Theory, ETH Zurich, CH-8093 Zürich, Switzerland*

[2]*Max Planck Institute for the Structure and Dynamics of Matter, DE-22761 Hamburg, Germany*

[3]*Institute for Materials Science, Los Alamos, New Mexico 87545, United States*

[4]*NORDITA, SE-106 91 Stockholm, Sweden*

[5]*Institute for Theoretical Studies, ETH Zurich, CH-8092 Zürich, Switzerland*

(Received 11 April 2017; published 19 June 2017)

An appealing mechanism for inducing multiferroicity in materials is the generation of electric polarization by a spatially varying magnetization that is coupled to the lattice through the spin-orbit interaction. Here we describe the reciprocal effect, in which a time-dependent electric polarization induces magnetization even in materials with no existing spin structure. We develop a formalism for this dynamical multiferroic effect in the case for which the polarization derives from optical phonons, and compute the strength of the phonon Zeeman effect, which is the solid-state equivalent of the well-established vibrational Zeeman effect in molecules, using density functional theory. We further show that a recently observed behavior—the resonant excitation of a magnon by optically driven phonons—is described by the formalism. Finally, we discuss examples of scenarios that are not driven by lattice dynamics and interpret the excitation of Dzyaloshinskii-Moriya-type electromagnons and the inverse Faraday effect from the viewpoint of dynamical multiferroicity.

DOI: 10.1103/PhysRevMaterials.1.014401

I. INTRODUCTION

Multiferroic materials, with their simultaneous magnetism and ferroelectricity, are of considerable fundamental and technological interest because of their cross-coupled magnetic and electric external fields and internal order parameters. Particularly intriguing are the class of multiferroics in which a noncentrosymmetric ordering of the magnetic moments induces directly a ferroelectric polarization. Prototypical examples are chromium chrysoberyl, Cr_2BeO_4 [1], in which the effect was first proposed, and terbium manganite, $TbMnO_3$, which provided the first modern example and detailed characterization [2,3]. The mechanism responsible for the induced ferroelectric polarization in these materials is the Dzyaloshinskii-Moriya interaction [4–7]: Electric polarization, $\mathbf{P} \sim \mathbf{M} \times (\nabla_\mathbf{r} \times \mathbf{M})$, emerges in spatial spin textures as a consequence of the lowest order coupling between polarization and magnetization, $\mathbf{P} \cdot [\mathbf{M} \times (\nabla_\mathbf{r} \times \mathbf{M})]$, in the usual Ginzburg-Landau picture [8–11].

From a symmetry point of view a reciprocal effect, in which magnetization is induced by ferroelectric polarization, must also exist. The time-reversal and spatial-inversion properties of magnetization and polarization—$\mathbf{M}$ is symmetric under space inversion and antisymmetric under time reversal, whereas $\mathbf{P}$ is symmetric under time reversal and antisymmetric under space inversion—indicate that the product $\mathbf{M} \cdot (\mathbf{P} \times \partial_t \mathbf{P})$ couples $\mathbf{M}$ and $\mathbf{P}$ at the same lowest order as $\mathbf{P} \cdot [\mathbf{M} \times (\nabla_\mathbf{r} \times \mathbf{M})]$. It follows that a magnetization

$$\mathbf{M} \sim \mathbf{P} \times \partial_t \mathbf{P} \tag{1}$$

develops in the presence of an appropriate dynamical polarization. This mechanism of induced magnetization by time-dependent polarization provides a dynamical analogy of the usual static multiferroicity. While the generation of polarization by spatial spin textures is now well established both experimentally and in first-principles calculations (see for example Refs. [12–15]), discussions of the reciprocal dynamical effect are scarce, perhaps surprisingly so, since the idea is rooted in the classical induction of a magnetic field by a circulating current. One notable example is the proposal that it is the cause of the observed paramagnetism and specific heat increase in a ferroelectric insulator [16,17]; this analysis has been largely unrecognized to date.

The purpose of this paper is to develop the formalism of this dynamical multiferroic effect and to describe observable effects that it leads to. We begin by deriving a formalism for magnetic moments induced by phonons that allows computation of their magnitudes using first-principles electronic structure calculations. This allows us to provide a general derivation of the phonon Zeeman effect as the solid-state equivalent to the well-established vibrational Zeeman effect in molecules and to analyze the limits under which the effect will be experimentally observable. Next, we give an explanation for a recently observed behavior, the resonant excitation of a magnon using optically driven phonons [18], in terms of dynamical multiferroicity. Finally we discuss the connection of dynamical multiferroicity to effects that are not related to lattice dynamics, specifically Dzyaloshinskii-Moriya-type electromagnons and the inverse Faraday effect.

Our investigation is particularly timely in light of recent progress in the ability to manipulate materials in the time domain to generate nonequilibrium states of matter with properties that differ from or are inaccessible in the static limit. Examples include the ultrafast structural phase transition in $(La,Ca)MnO_3$ driven by melting of orbital order [19] and the report of enhanced superconducting transition temperature in the high-T_c cuprate yttrium barium copper oxide [20–22]. In addition, a number of theoretical proposals exist, for example predictions within Floquet theory of emerging topological states [23], and of temporal control of spin currents [24]. Our work in turn contributes to this growing field of "dynamical materials design" by providing an additional mechanism—time-dependence of polarization—through which novel states can be dynamically generated.

*dominik.juraschek@mat.ethz.ch

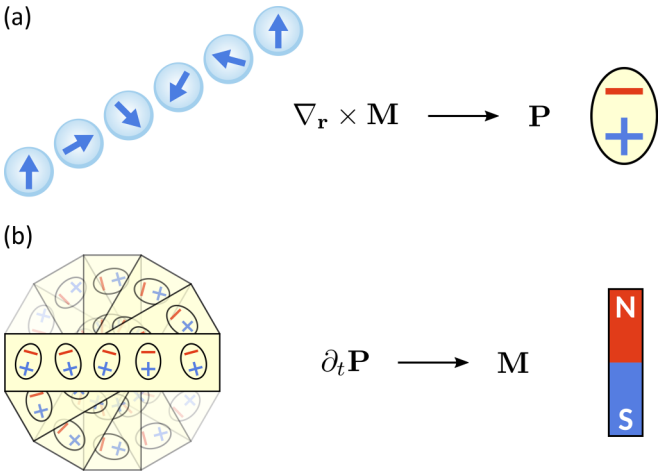

FIG. 1. Duality of magnetization and polarization. (a) A spatially varying magnetization induces a polarization, as is well known for example in multiferroic $TbMnO_3$ [2,3,8,10]. (b) A temporally varying polarization induces a magnetization as shown in this work.

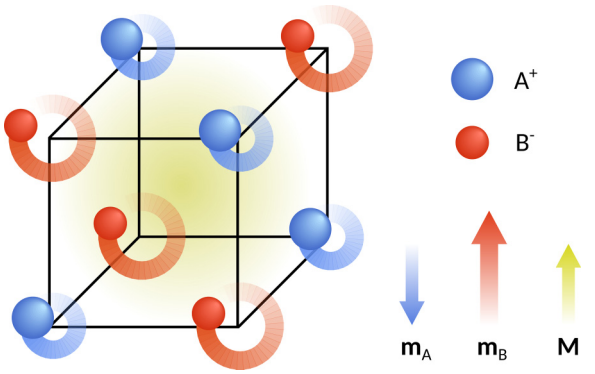

FIG. 2. Magnetic moments from ionic loops. Schematic motion of ions in a diatomic A^+B^- material driven by perpendicular optical phonons. The circular motions of the ions create local magnetic moments, $\mathbf{m}_A$ and $\mathbf{m}_B$. The area covered by the ionic loop of the lighter ion (here B^-) is larger, and therefore its local magnetic moment overcompensates that of the heavier ion. This leads to a macroscopic magnetic moment, $\mathbf{M}$.

II. FORMALISM FOR DYNAMICAL MULTIFERROICITY

We begin by reviewing the duality between the time dependence of $\mathbf{P}$ and spatial gradient of $\mathbf{M}$ that we discussed in the introduction and that is illustrated in Fig. 1. A spatially varying magnetic structure induces a ferroelectric polarization; if the gradient is zero, the polarization vanishes. Both the sense of the spin spiral and the direction of polarization persist statically in one of two degenerate ground states: If the sense of the spin spiral is reversed, the polarization inverts. In the case of the dynamical multiferroic effect, a temporally varying polarization induces a magnetization; if the time derivative is zero, the magnetization vanishes. Here, both the sense of the rotating polarization (i.e., the curl of $\mathbf{P} \times \partial_t \mathbf{P}$) and the direction of the magnetization persist *dynamically* in one of two degenerate ground states of the dynamical system: If the sense of the rotating polarization is inverted, the magnetization reverses. A quasistatic state of the magnetization is realized when the rotation of the polarization is steady. The induced magnetization can then couple to lattice and magnetic degrees of freedom of the system, as we will show in various examples. We emphasize that magnetism can be induced by a time-varying polarization in a previously nonmagnetic system, just as a spatially varying magnetization can induce a polarization in a system that is previously nonpolar.

For the general case of a magnetization induced by two perpendicular dynamical polarizations that are oscillating sinusoidally with frequencies ω_1 and ω_2 and a relative phase shift of φ, we write the time-dependent polarization as

$$\mathbf{P}(t) = \begin{pmatrix} P_1(t) \\ P_2(t) \end{pmatrix} = \begin{pmatrix} A_1 \sin(\omega_1 t + \varphi) \\ A_2 \sin(\omega_2 t) \end{pmatrix}, \tag{2}$$

where one of the components can, in principle, also be static (ω_1 or ω_2 equal to zero). Evaluating Eq. (1) with this polarization we obtain

$$\mathbf{M}(t) \sim \left[\frac{\omega_+}{2} \sin(\omega_- t + \varphi) - \frac{\omega_-}{2} \sin(\omega_+ t + \varphi) \right] A_1 A_2 \hat{z}. \tag{3}$$

A time-varying magnetization is induced that is oriented perpendicular to the spatial orientations of both polarizations. The magnetization consists of a superposition of a large-amplitude oscillation with the difference frequency, $\omega_- = \omega_1 - \omega_2$, and a small-amplitude oscillation with the sum frequency, $\omega_+ = \omega_1 + \omega_2$. If the frequencies are equal, $\omega_1 = \omega_2$, the induced magnetization is static.

III. DYNAMICAL MULTIFERROICITY MEDIATED BY PHONONS

The polar nature of optical phonons means that they can induce time-dependent polarization, and in turn dynamical multiferroicity, in materials. We write the polarization, $\mathbf{P}$, caused by the displacing atoms in a normal-mode vibration as the Born effective charges, $\mathbf{Z}^*$, of the ions multiplied by the normal coordinates, $\mathbf{Q}$, of the phonon modes, $\mathbf{P} = \mathbf{Z}^*\mathbf{Q}$. (Note that another approach is to use a Berry phase calculation; this was shown to lead to similar results [25,26].) The connection to the usual relation between magnetic moment and angular momentum [27] is revealed by rewriting Eq. (1) to obtain

$$\mathbf{M} = \gamma \mathbf{Q} \times \dot{\mathbf{Q}} = \gamma \mathbf{L}, \tag{4}$$

where γ is a gyromagnetic ratio and $\mathbf{L} = \mathbf{Q} \times \dot{\mathbf{Q}}$ an angular momentum. Optical phonons with perpendicular polarity induce circular motions of the ions (ionic loops) whose individual magnetic moments combine to produce an effective macroscopic magnetic moment, as depicted in Fig. 2. The direction of $\mathbf{M}$ is determined by the sense of the ionic loop. The magnetic moment of phonons is the solid-state equivalent of the vibrational magnetic moment of molecules [28].

For a many-body system, such as a phonon, the simple tensorial relation of Eq. (4) is generally more complex. The total magnetic moment per unit cell is given by the sum of the moments caused by the circular motion of each ion [29]:

$$\mathbf{M} = \sum_i \mathbf{m}_i = \sum_i \gamma_i \mathbf{L}_i. \tag{5}$$

Here $\mathbf{m}_i$ is the magnetic moment of ion i, $\mathbf{L}_i$ its angular momentum, and γ_i its gyromagnetic ratio, and the sum is over all ions in one unit cell. The angular momentum results from the motion of the ion along the eigenvectors of all contributing phonon modes [30]:

$$\mathbf{L}_i = \sum_{\alpha,\beta} \mathbf{Q}_{i\alpha} \times \dot{\mathbf{Q}}_{i\beta} = \sum_{\alpha,\beta} Q_\alpha \dot{Q}_\beta \mathbf{q}_{i\alpha} \times \mathbf{q}_{i\beta}, \tag{6}$$

where we wrote the displacement vector of ion i corresponding to mode α, $\mathbf{Q}_{i\alpha}$, in terms of a product of the normal mode coordinate amplitude, Q_α, with the unit eigenvector, $\mathbf{q}_{i\alpha}$: $\mathbf{Q}_{i\alpha} = Q_\alpha \mathbf{q}_{i\alpha}$. Indices α and β run over all contributing phonon modes. The gyromagnetic ratio tensor is the effective charge to mass ratio of the ion:

$$\gamma_i = \frac{e\mathbf{Z}_i^*}{2M_i}, \tag{7}$$

where $\mathbf{Z}_i^*$ is the Born effective charge tensor of ion i and M_i its mass.

We will now rewrite the magnetic moment of Eq. (5) in terms of the phononic system. We insert the expression for the angular momentum of Eq. (6) in Eq. (5) to obtain

$$\begin{aligned}\mathbf{M} &= \sum_i \gamma_i \sum_{\alpha,\beta} Q_\alpha \dot{Q}_\beta \mathbf{q}_{i\alpha} \times \mathbf{q}_{i\beta} \\ &= \sum_{\alpha<\beta} (Q_\alpha \dot{Q}_\beta - Q_\beta \dot{Q}_\alpha) \sum_i \gamma_i \mathbf{q}_{i\alpha} \times \mathbf{q}_{i\beta}.\end{aligned} \tag{8}$$

Now we write the difference of the normal mode coordinates as an angular momentum, analogously to Eq. (6):

$$(Q_\alpha \dot{Q}_\beta - Q_\beta \dot{Q}_\alpha) = \mathbf{Q}_{\alpha\beta} \times \dot{\mathbf{Q}}_{\alpha\beta} = \mathbf{L}_{\alpha\beta}, \tag{9}$$

where $\mathbf{Q}_{\alpha\beta}$ contains the normal coordinates of the modes α and β in the basis of their symmetric representation. The remaining part of $\mathbf{M}$ resembles a gyromagnetic ratio; therefore we write Eq. (8) as

$$\mathbf{M} = \sum_{\alpha<\beta} \gamma_{\alpha\beta} \mathbf{L}_{\alpha\beta} = \sum_{\alpha<\beta} \mathbf{m}_{\alpha\beta}, \tag{10}$$

where

$$\gamma_{\alpha\beta} = \sum_i \gamma_i \mathbf{q}_{i\alpha} \times \mathbf{q}_{i\beta} \tag{11}$$

is the gyromagnetic ratio vector and $\mathbf{L}_{\alpha\beta}$ the angular momentum of a system of phonons. The induced magnetic moments, $\mathbf{m}_{\alpha\beta}$, are generated by the ionic loops caused by pairs of phonon modes, α and β. For only two contributing phonon modes Eq. (10) reduces to the simple tensorial form

$$\mathbf{M} = \mathbf{m}_{12} = \gamma_{12} \mathbf{L}_{12} = \gamma_{12} \mathbf{Q}_{12} \times \dot{\mathbf{Q}}_{12}. \tag{12}$$

We note that all quantities in this section, particularly the Born effective charge tensors, $\mathbf{Z}_i^*$, and the phonon eigenvectors, $\mathbf{q}_{i\alpha}$, can be calculated from first principles using standard density functional theory methods.

A. Phonon Zeeman effect

Next we discuss the Zeeman splitting of degenerate phonon modes, building on the early work extending the well-established vibrational Zeeman effect in molecules [31] to solids [32,33], as well as a derivation for cubic perovskites [26] and a phenomenological analysis [16]. Here we derive a general formalism for the phonon Zeeman effect that is amenable to computation using density functional theory via the quantities defined in the previous section.

Consider two degenerate phonon modes ($\omega_1 = \omega_2 = \omega_0$) polarized along perpendicular axes and shifted in phase by $\varphi \neq 0$. Equation (3) then reduces to

$$\mathbf{M}(0) \sim \omega_0 \sin(\varphi) A_1 A_2 \hat{z}. \tag{13}$$

We see that the magnetization induced by the atomic motions is static and its magnitude depends only on the amplitude of the lattice vibrations, on their frequency, and on the phase shift between the two sinusoidal fields, reaching a maximum at $\varphi = \pi/2$. If an external magnetic field, $\mathbf{B}$, is applied to the system, this induced magnetization interacts with it via the usual Zeeman coupling, with the result that the degeneracy of the phonon modes is lifted.

The Lagrangian describing the interaction of this magnetic moment with an externally applied magnetic field is

$$\mathcal{L}(\mathbf{Q},\dot{\mathbf{Q}}) = \frac{1}{2}|\dot{\mathbf{Q}}|^2 - \frac{\omega^2}{2}|\mathbf{Q}|^2 + \mathbf{B}\cdot\mathbf{M}, \tag{14}$$

where $\mathbf{B}$ is the external magnetic field, $\mathbf{Q} = \mathbf{Q}_{12} = (Q_1, Q_2, 0)$ contains the normal coordinates of two degenerate phonon modes, and $\mathbf{M}$ is their magnetic moment as in Eq. (12). We can write the Lagrangian component-wise as

$$\begin{aligned}\mathcal{L}(Q_1,Q_2,\dot{Q}_1,\dot{Q}_2) = \frac{1}{2}\dot{Q}_1^2 + \frac{1}{2}\dot{Q}_2^2 - \frac{\omega^2}{2}Q_1^2 - \frac{\omega^2}{2}Q_2^2 \\ + \gamma B_z (Q_1\dot{Q}_2 - Q_2\dot{Q}_1),\end{aligned} \tag{15}$$

where $\gamma = \gamma_{12}$ is the gyromagnetic ratio as derived in Eqs. (11) and (12), and B_z is the z component of the magnetic field. After a Fourier transformation,

$$Q_\alpha \to Q_\alpha = Q_{\alpha\omega} e^{i\omega t}, \tag{16}$$

$$Q_\alpha^2 \to Q_{\alpha\omega} Q_{\alpha\omega}^*, \tag{17}$$

$$Q_\alpha \dot{Q}_\beta \to \tfrac{1}{2}(Q_{\alpha\omega}\dot{Q}_{\beta\omega}^* + Q_{\alpha\omega}^* \dot{Q}_{\beta\omega}), \tag{18}$$

the Lagrangian becomes

$$\mathcal{L}(\mathbf{Q}_\omega, \mathbf{Q}_\omega^*) = \mathbf{Q}_\omega \mathbf{A} \mathbf{Q}_\omega^*, \tag{19}$$

where $\mathbf{Q}_\omega = (Q_{1\omega}, Q_{2\omega}, 0)$ contains the normal mode coordinates in Fourier space, and

$$\mathbf{A} = \begin{pmatrix} \omega^2 - \omega_0^2 & 2i\gamma B_z \omega \\ -2i\gamma B_z \omega & \omega^2 - \omega_0^2 \end{pmatrix}. \tag{20}$$

We solve the determinant for the zone center ($\omega \to \omega_0$) and obtain a splitting of the degenerate phonon modes:

$$\omega = \omega_0 \sqrt{1 \pm \frac{2\gamma B}{\omega_0}} \approx \omega_0 \pm \gamma B_z. \tag{21}$$

The splitting is sketched in Fig. 3 for a magnetic moment aligned parallel and antiparallel to an external field, corresponding to a left- and right-handed sense of the phonons. Notably the phonon Zeeman effect is independent of the magnitude of the phonon magnetic moment and hence the

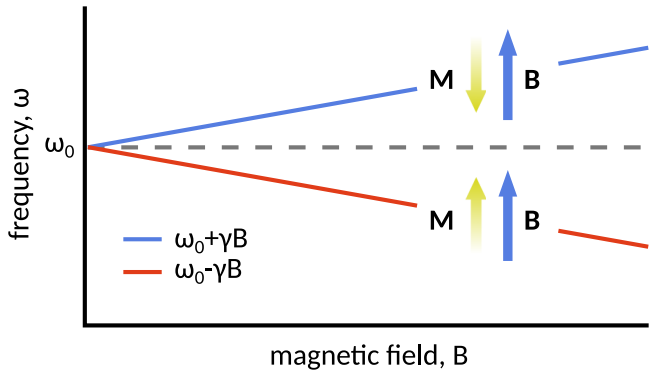

FIG. 3. Zeeman splitting of degenerate phonon modes. Sketch of the phonon Zeeman splitting as a function of the external magnetic field **B**. The phonons with their magnetic moment **M** aligned parallel to the external magnetic field **B** has a lower energy than the phonons with their moment aligned antiparallel to the field.

amplitude of the lattice vibrations. It is therefore present in optical modes excited, for example thermally or due to zero-point fluctuations [16,34], and does not require intense optical pumping.

We estimate the magnitude of the effect for the tetragonal phase of strontium titanate, $SrTiO_3$, using density functional theory. (Please see the "Computational methods for phonon calculations" section for details of the calculation.) Our calculated low-frequency degenerate E_g phonon modes lie at 1 THz, and their gyromagnetic ratio as calculated with Eq. (11) is $\gamma = 0.9 \times 10^7\ \mathrm{T}^{-1}\ \mathrm{s}^{-1}$. (Note that the g factor obtained in Ref. [25] for cubic $SrTiO_3$ using the Berry phase approach has a similar value.) It follows that to obtain a relative splitting of the eigenfrequency of $2\gamma B/\omega_0 \approx 10^{-3}$ one needs a magnetic field of the order of $B = 55$ T; at this field strength, our splitting is four orders of magnitude larger than the value estimated in Ref. [35] for the splitting of *acoustic* phonons. While the splitting for $SrTiO_3$ is small, the effect will be significantly enhanced in materials with high Born effective charges, light ions, and low-frequency optical phonon modes. Promising candidates are ABO_3 compounds in which a heavy A/B-site ion ensures low-frequency phonons, while the light B/A-site ion and the oxygens make up a large percentage of the motion in the normal mode. A further approach to increasing the magnitude of the effect is to identify materials with dynamically varying Born effective charges which will lead to an additional contribution to the angular momentum proportional to $(\partial_t \mathbf{Z}^*)\mathbf{Q}$.

B. Resonant magnon excitation by optically driven phonons

A recently observed example of the dynamical multiferroic effect is the resonant excitation of magnons through the frequency-dependent magnetic moment of a system of phonons. Consider two nondegenerate phonon modes ($\omega_1 \neq \omega_2$) with perpendicular polarity. Setting $\varphi = 0$ without loss of generality, Eq. (3) then reduces to

$$\mathbf{M}(t) \sim \left[\frac{\omega_+}{2}\sin(\omega_- t) - \frac{\omega_-}{2}\sin(\omega_+ t)\right] A_1 A_2 \hat{z}. \qquad (22)$$

We obtain an induced magnetization that varies in time as a superposition of a large-amplitude oscillation with the difference frequency, ω_-, and a small-amplitude oscillation with the sum frequency, ω_+.

Such a situation was recently realized experimentally by applying an intense linearly polarized terahertz pulse along the [110] direction in the a-b plane of orthorhombic perovskite-structure erbium ferrite, $ErFeO_3$ [18]. The pulse drives the high-frequency IR-active phonon modes B_{3u} and B_{2u} with polarization along the a and b lattice vectors. Due to the $Pbnm$ symmetry of $ErFeO_3$, these modes have slightly different eigenfrequencies (17.0 and 16.2 THz). Intriguingly, the spontaneous excitation of a magnon at 0.75 THz, close to the difference frequency, was observed. Our analysis above indicates that this behavior is a manifestation of the dynamical multiferroic effect: The large-amplitude part of the induced magnetic moment, **M**, oscillates with the difference frequency $\omega_- = 0.8$ THz, sufficiently close to the 0.75 THz magnon of $ErFeO_3$ [36], which is thus resonantly excited by **M**.

Indeed a dynamical simulation of the evolution of the phonons with parameters computed from density functional theory confirms the behavior predicted phenomenologically in Eq. (22). (See the "Computational methods for phonon calculations" section for details of the calculation.) In Fig. 4(a) we show the induced magnetic moment as calculated by Eq. (10) and in Fig. 4(b) the normal mode coordinate of the high-frequency IR-active B_{3u} and B_{2u} modes following an excitation with an ultrashort terahertz pulse. The small-amplitude oscillation of **M** with the sum frequency is negligible and only the large-amplitude oscillation with the difference frequency contributes. The induced magnetic moment peaks at the order of magnitude of the nuclear magneton with $|\mathbf{M}| \approx 0.1\mu_N$ per unit cell. It decays together with the IR modes over the time scale of a few picoseconds; experimentally the induced magnon was found to survive for at least 35 ps [18].

While the phonon Zeeman effect is independent of the magnitude of the phonon magnetic moment, the resonant effect discussed here is quadratic in the amplitude of the dynamical polarization and therefore dependent on the intensity of the exciting terahertz pulse. At high pulse intensities an anharmonic coupling of the excited IR phonons to Raman-active phonons was shown to be relevant in $ErFeO_3$ [37]. These modes do not contribute to the gyromagnetic ratio however, and we can therefore neglect the effect of nonlinear phononics in the above analysis.

C. Computational methods for phonon calculations

We calculated the phonon eigenfrequencies and eigenvectors and the Born effective charges of $SrTiO_3$ and $ErFeO_3$ from first principles using the density functional theory formalism as implemented in the Vienna *ab initio* simulation package (VASP) [38,39] and the frozen-phonon method as implemented in the PHONOPY package [40]. We used the default VASP PAW pseudopotentials with Er $4f$ electrons treated as core states. We converged the Hellmann-Feynman forces to 10^{-5} eV/Å using a plane-wave energy cutoff of 700 eV and a $7 \times 7 \times 5$ k-point mesh to sample the Brillouin zone for $SrTiO_3$ and 850 eV, $6 \times 6 \times 4$ for $ErFeO_3$. For the exchange-correlation functional we chose the PBEsol [41]

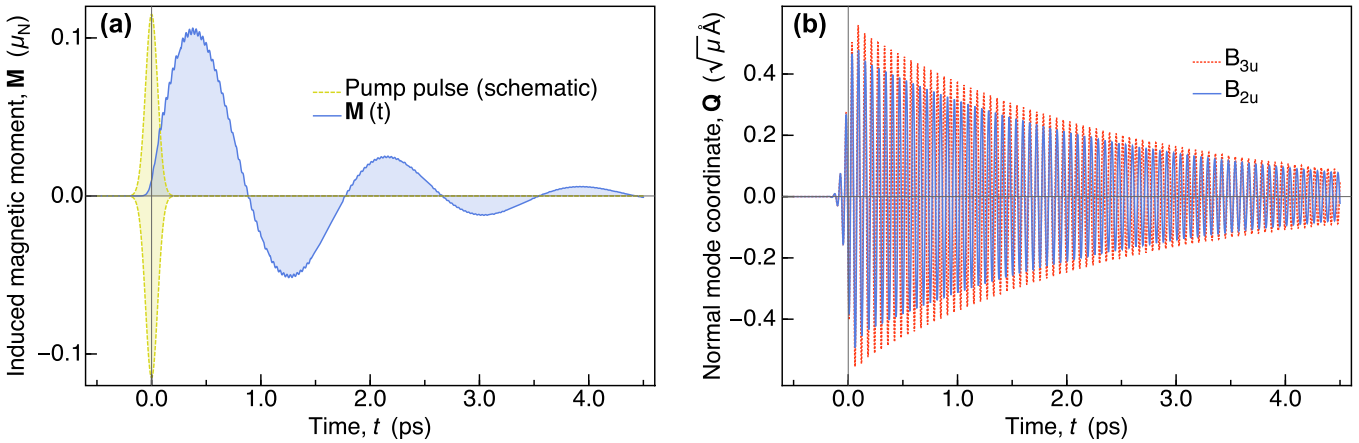

FIG. 4. Calculated time-varying magnetic moment from optically driven phonons in $ErFeO_3$. (a) Time evolution of the phonon magnetic moment $\mathbf{M}$ in units of the nuclear magneton μ_N in $ErFeO_3$ after excitation with an ultrashort terahertz pulse. The phonon magnetic moment oscillates with a large amplitude with the difference frequency, $\omega_- = \omega_1 - \omega_2$, and with a small amplitude with the sum frequency, $\omega_+ = \omega_1 + \omega_2$. The schematic pump pulse has a duration of 130 fs. (b) Time evolution of the normal mode coordinates Q_α of the excited high-frequency IR modes ($\alpha = B_{3u}, B_{2u}$) in units of $\sqrt{\mu}$Å, where μ is the atomic mass unit.

form of the generalized gradient approximation (GGA) and imposed a Hubbard correction of $U = 3.7$ eV and a Hund's exchange of $J = 0.7$ eV on the Fe $3d$ states in $ErFeO_3$. Our fully relaxed structures with lattice constants $a = 5.51$ Å and $c = 7.77$ Å for $SrTiO_3$ and $a = 5.19$ Å, $b = 5.56$ Å, and $c = 7.52$ Å for $ErFeO_3$ fit reasonably well the experimental values of Refs. [42,43], as do our calculated phonon eigenfrequencies [18,36,44–46]. Our calculated values for the highest IR phonon frequencies are 16.52 THz for the B_{3u} and 15.95 THz for the B_{2u} mode in $ErFeO_3$. For the time evolution of IR phonons after a pulsed optical excitation, we obtain the time-dependent normal mode coordinates, Q, by numerically solving the dynamical equations of motion:

$$\ddot{Q}_\alpha + \kappa_\alpha \dot{Q}_\alpha + \omega_\alpha^2 Q_\alpha = F, \tag{23}$$

where κ_α is the friction coefficient and ω_α the eigenfrequency of mode α. We used a realistic friction of a twentieth of the eigenfrequency. The periodic driving force F models the terahertz pulse in a realistic fashion with Gaussian shape with an amplitude of 10 MV cm^{-1}, and a finite width in both time (FWHM = 130 fs) and frequency (peak frequency 19.5 THz, FWHM = 6.5 THz) [18].

IV. BEYOND LATTICE DYNAMICS

In the previous two examples we showed how the magnetic moment arising from a system of phonons couples lattice and magnetic degrees of freedom. In the following we discuss examples in which the time-dependent polarization is not caused by lattice dynamics.

A. Dzyaloshinskii-Moriya-type electromagnons

The existence of electromagnons—that is spin waves excited by ac electric fields—was demonstrated ten years ago in multiferroic materials with an incommensurate (cycloidal or helicoidal) magnetic structure [47]. In the original report, the interaction was shown to be mediated through conventional Heisenberg coupling of spins, leading to a phonon-magnon hybridization that makes the magnon electroactive (and is therefore called an electromagnon) [47–54]. A second mechanism for generating electromagnons, in which electroactive excitation of the spin spiral occurs via the Dzyaloshinskii-Moriya interaction, has also been identified [54–59]. We show in the following that the description of these electromagnons from the viewpoint of dynamical multiferroicity is equivalent to the previously introduced formalism via the inverse effect of the Dzyaloshinskii-Moriya interaction [55].

The standard description of a Dzyaloshinskii-Moriya-type electromagnon in a helical magnet is through the coupling of the spin degrees of freedom of the cycloid, $\mathbf{S}_m$, with a uniform lattice displacement, $\mathbf{u}$. The ferroelectric polarization is given by $\mathbf{P}_{FE} \propto \mathbf{e}_{ij} \times (\mathbf{S}_i \times \mathbf{S}_j)$, where $\mathbf{e}_{ij}$ is the vector connecting the sites i and j. The component n of the lattice displacement that couples to the rotation of the spin plane is parallel to its rotation axis, $\mathbf{u}^n \| (\mathbf{S}_i \times \mathbf{S}_j)$. An ac electric field, $\mathbf{E} \| \mathbf{u}^n$, then induces a magnetization, $\mathbf{m} \| \mathbf{e}_{ij}$, and excites an electromagnon when it matches the frequency of the eigenmode of the spin cycloid [55]. Specifically in $TbMnO_3$ with a magnetic field applied along b, the spin cycloid lies in the a-b plane. Since $(\mathbf{S}_i \times \mathbf{S}_j) \| c$ and $\mathbf{e}_{ij} \| b$, the resulting $\mathbf{P}_{FE} \| a$. The ac electric field component of subterahertz radiation, $\mathbf{E} \| c$, then induces a magnetization, $\mathbf{m} \| b$, and excites a Dzyaloshinskii-Moriya-type electromagnon when it matches the eigenfrequency of the spin cycloid at 0.63 THz [57]. To disentangle this clutter of alignments, we illustrate the symmetry in Fig. 5. Note that a cooperative contribution of the ferroelectric polarization from symmetric magnetostriction has been reported [60,61], which, however, leaves our symmetry analysis here unaffected.

This situation is exactly consistent with the formalism of dynamical multiferroicity when the two perpendicular polarizations in Eq. (2) are given by $\mathbf{P} = (P_1(0), 0, P_2(t))$, where $P_1(0) \equiv \mathbf{P}_{FE}$ ($\omega_1 = 0$, $\varphi = \pi/2$) and $P_2(t) \equiv \mathbf{E}(t)$ ($\omega_2 = \omega_0$). Equation (3) then reduces to

$$\mathbf{M}(t) \sim \omega_0 \cos(\omega_0 t) A_1 A_2 \hat{y}. \tag{24}$$

The formalism predicts an induced magnetization that oscillates with the frequency of the terahertz radiation, ω_0,

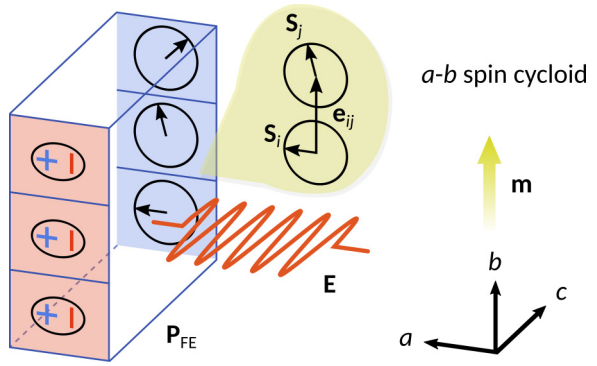

FIG. 5. Dzyaloshinskii-Moriya-type electromagnon symmetry in $TbMnO_3$. Spin cycloid oriented in the a-b plane with ferroelectric polarization $\mathbf{P}_{FE}$ along a. To excite a Dzyaloshinskii-Moriya electromagnon, the ac electric field of the subterahertz radiation $\mathbf{E}$ has to be aligned along c and the induced magnetization $\mathbf{m}$ is along b.

identical to the magnetization described above within the inverse Dzyaloshinskii-Moriya formalism, $\mathbf{M}(t) \equiv \mathbf{m}$.

B. Inverse Faraday effect

Finally, we show that the inverse Faraday effect, which describes the generation of a static magnetization in a material when irradiated with circularly polarized light, can also be interpreted from the viewpoint of dynamical multiferroicity. The inverse Faraday effect was first demonstrated in the 1960s [62–64] and experienced a massive revival in the last decade, after it was shown that it can be used to control magnetization nonthermally with photomagnetic pulses [65]. The standard description of the effect is

$$\mathbf{M}(\omega) = \chi(\omega)\mathbf{E}(\omega) \times \mathbf{E}^*(\omega), \tag{25}$$

where $\mathbf{M}$ is the induced magnetization, χ the magneto-optic susceptibility, and $\mathbf{E}$ the electric field component of the circularly polarized light. The electric field induces perpendicular time-varying polarizations in the material and the connection to dynamical multiferroicity is revealed by rewriting Eq. (25) in the time domain:

$$\begin{aligned}\mathbf{M}(t) &= \chi(t)\mathbf{E}(t) \times \partial_t \mathbf{E}(t) \\ &\sim \mathbf{P} \times \partial_t \mathbf{P}.\end{aligned} \tag{26}$$

The perpendicular time-dependent polarizations induced by the circularly polarized light both oscillate with the frequency of the light ($\omega_1 = \omega_2 = \omega_0$) and are shifted in phase by $\varphi = \pi/2$. Equation (3) therefore reproduces the induced static magnetization of the inverse Faraday effect:

$$\mathbf{M}(0) \sim \omega_0 A_1 A_2 \hat{z}. \tag{27}$$

Note that the investigation of the inverse Faraday effect has been extended in recent years by microscopic theories [66] that also describe ultrafast time scales [67,68], as well as the case of linearly polarized light [69]; these extensions are beyond the scope of the analogy provided here.

V. DISCUSSION

In summary, we have introduced the concept of dynamical multiferroicity and shown that it provides a straightforward unifying interpretation of four diverse phenomena, summarized in Table I: (i) the Zeeman splitting of phonon spectra in a magnetic field, (ii) resonant magnon scattering, (iii) electromagnon coupling, and (iv) the inverse Faraday effect. In the case of (i) and (ii), in which the multiferroicity is mediated by lattice dynamics, we showed that the dynamical multiferroic coupling can be calculated quantitatively using standard density functional theory methods, and we performed such calculations for representative materials in each case.

Since the term *nonlinear* is used in both optics (for example second-harmonic generation) and phononics (for example cubic and higher-order phonon-phonon interactions), we also clarify the order (linear or higher order and in which parameter) of the excitations for the four cases. First, in the cases of $SrTiO_3$, $ErFeO_3$, and $DyFeO_3$, the materials are centrosymmetric, so a nonlinear second-harmonic optical response to the terahertz pulse is not possible. In the case of $TbMnO_3$, second-harmonic generation occurs at higher energies than the sub-THz radiation used in the example

TABLE I. Summary of examples for the dynamical multiferroic effect. The table shows the frequency of the induced magnetic moment, $\mathbf{M}(t)$, the type of excitation, the type of drive, and the order of the effect in terms of the time-dependent polarization, $P(t)$, for the four examples discussed in this work. From left to right: Phonon Zeeman effect in $SrTiO_3$, resonant magnon excitation by optically driven phonons in $ErFeO_3$, Dzyaloshinskii-Moriya-type electromagnon in $TbMnO_3$, and the inverse Faraday effect in $DyFeO_3$.

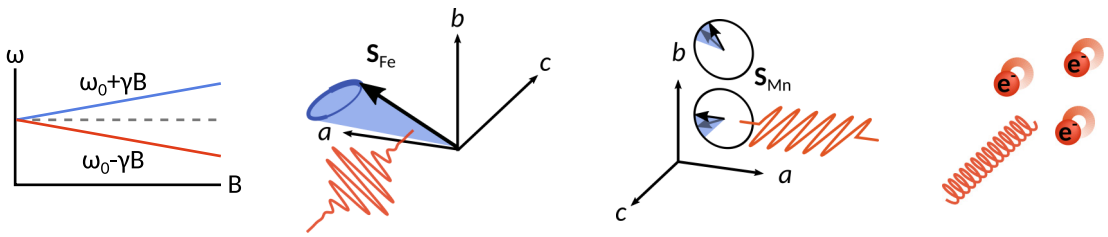

Example material	$SrTiO_3$	$ErFeO_3$	$TbMnO_3$	$DyFeO_3$
$\mathbf{M}(t)$ frequency	static	$\omega_1 - \omega_2$	ω_0	static
Excitation	thermal, zero-point	THz	sub-THz	IR
Polarization of drive		linear	linear	circular
Order of $P(t)$		quadratic	linear	quadratic

(see for example Ref. [70]). In addition, while cubic and higher-order nonlinear phononic coupling has indeed been demonstrated in some of these materials (see, for example, Ref. [37] for a detailed analysis in the case of $ErFeO_3$), the phenomena described here are not driven by nonlinear phononic effects. The phonon Zeeman effect in $SrTiO_3$ is independent of the amplitude of the degenerate phonons and requires no external excitation and so is zeroth order in the polarization amplitude. The magnon excitation in $ErFeO_3$ depends on the quadratic term in the phonon amplitude and so is nonlinear in the amplitude of the driven time-dependent polarization, $P(t)$. As for the Dzyaloshinskii-Moriya-type electromagnon excitation, the induced magnetization is *linear* in $P(t)$ (with the perpendicular ferroelectric polarization being static), while the inverse Faraday effect is nonlinear in $P(t)$ due to the excitation with circularly polarized light.

The phonon Zeeman splitting that we analyze here is distinct from previously discussed interactions between phonons and magnetism in *magnetic* materials. These include the phonon angular momentum arising from spin-phonon interaction [71], the splitting of acoustic phonons due to the spin-orbit interaction [72], the splitting of nondegenerate Raman-active phonon modes accompanying a ferroelectric to paraelectric phase transition [73], and the magnetic-field dependence of the phonon frequencies in Ce compounds [74–76]. In contrast, the phonon Zeeman effect does not require magnetic ions. The report of a splitting of degenerate phonons due to the interaction with magnetoexcitons in graphene [77] is a fascinating phenomenon, but also a different mechanism from the phonon Zeeman effect. It is further distinct from the phonon Hall effect proposed for acoustic phonons as an analog of the anomalous Hall effect [78,79].

With the increased availability of intense THz sources of radiation, we anticipate that additional manifestations of dynamical multiferroicity will be revealed over the next years. Reciprocally, we expect that the effect will be used to engineer new behaviors that are not accessible in the static domain. In this context, we point out that dynamical multiferroicity provides a unit-cell analog of an electric motor, in which the time-dependent polarization acts as a nanoscale electromagnetic coil to generate magnetic fields. This analogy might open a pathway to unforeseen technological applications.

ACKNOWLEDGMENTS

We thank G. Aeppli, A. Cavalleri, M. Fiebig, T. F. Nova, and A. Scaramucci for useful discussions. This work was supported by the ETH Zürich, by Dr. Max Rössler and the Walter Haefner Foundation through the ETH Zürich Foundation, by US DOE E3B7, and by the ERC Advanced Grant program No. 291151 and No. DM-321031. Calculations were performed at the Swiss National Supercomputing Centre (CSCS) supported by the project IDs s624 and p504.

[1] R. E. Newnham, J. J. Kramer, W. E. Schulze, and L. E. Cross, Magnetoferroelectricity in Cr_2BeO_4, J. Appl. Phys. **49**, 6088 (1978).

[2] T. Kimura, T. Goto, H. Shintani, K. Ishizaka, T. Arima, and Y. Tokura, Magnetic control of ferroelectric polarization, Nature (London) **426**, 55 (2003).

[3] M. Kenzelmann, A. B. Harris, S. Jonas, C. Broholm, J. Schefer, S. B. Kim, C. L. Zhang, S. W. Cheong, O. P. Vajk, and J. W. Lynn, Magnetic Inversion Symmetry Breaking and Ferroelectricity in $TbMnO_3$, Phys. Rev. Lett. **95**, 087206 (2005).

[4] I. E. Dzyaloshinskii, Thermodynamic theory of "weak" ferromagnetism in antiferromagnetic substances, J. Exptl. Theoret. Phys. (U.S.S.R.) **32**, 1547 (1957) [Sov. Phys. JETP **5**, 1259 (1957)].

[5] I. E. Dzyaloshinskii, Thermodynamic theory of "weak" ferromagnetism in antiferromagnetics, J. Phys. Chem. Solids **4**, 241 (1958).

[6] T. Moriya, New Mechanism of Anisotropic Superexchange Interaction, Phys. Rev. Lett. **4**, 228 (1960).

[7] T. Moriya, Anisotropic superexchange interaction and weak ferromagnetism, Phys. Rev. **120**, 91 (1960).

[8] H. Katsura, N. Nagaosa, and A. V. Balatsky, Spin Current and Magnetoelectric Effect in Noncollinear Magnets, Phys. Rev. Lett. **95**, 057205 (2005).

[9] I. A. Sergienko and E. Dagotto, Role of the Dzyaloshinskii-Moriya interaction in multiferroic perovskites, Phys. Rev. B **73**, 094434 (2006).

[10] M. Mostovoy, Ferroelectricity in Spiral Magnets, Phys. Rev. Lett. **96**, 067601 (2006).

[11] S.-W. Cheong and M. Mostovoy, Multiferroics: A magnetic twist for ferroelectricity, Nat. Mater. **6**, 13 (2007).

[12] Y. Yamasaki, H. Sagayama, T. Goto, M. Matsuura, K. Hirota, T. Arima, and Y. Tokura, Electric Control of Spin Helicity in a Magnetic Ferroelectric, Phys. Rev. Lett. **98**, 147204 (2007).

[13] A. Malashevich and D. Vanderbilt, First-Principles Study of Improper Ferroelectricity in $TbMnO_3$, Phys. Rev. Lett. **101**, 037210 (2008).

[14] R. Kajimoto, H. Sagayama, K. Sasai, T. Fukuda, S. Tsutsui, T. Arima, K. Hirota, Y. Mitsui, H. Yoshizawa, A. Q R Baron, Y. Yamasaki, and Y. Tokura, Unconventional Ferroelectric Transition in the Multiferroic Compound $TbMnO_3$ Revealed by the Absence of an Anomaly in *c*-Polarized Phonon Dispersion, Phys. Rev. Lett. **102**, 247602 (2009).

[15] H. C. Walker, F. Fabrizi, L. Paolasini, and F. de Bergevin, Femtoscale magnetically induced lattice distortions in multiferroic $TbMnO_3$, Science **333**, 1273 (2011).

[16] I. E. Dzyaloshinskii and D. L. Mills, Intrinsic paramagnetism of ferroelectrics, Philos. Mag. **89**, 2079 (2009).

[17] J. C. Lashley, M. F. Hundley, B. Mihaila, J. L. Smith, C. P. Opeil, T. R. Finlayson, R. A. Fisher, and N. Hur, Heat capacity in magnetic and electric fields near the ferroelectric transition in triglycine sulfate, Appl. Phys. Lett. **90**, 052910 (2007).

[18] T. F. Nova, A. Cartella, A. Cantaluppi, M. Först, D. Bossini, R. V. Mikhaylovskiy, A. V. Kimel, R. Merlin, and A. Cavalleri, An effective magnetic field from optically driven phonons, Nat. Phys. **13**, 132 (2017).

[19] P. Beaud, S. L. Johnson, E. Vorobeva, U. Staub, R. A. De Souza, C. J. Milne, Q. X. Jia, and G. Ingold, Ultrafast Structural Phase Transition Driven by Photoinduced Melting of Charge and Orbital Order, Phys. Rev. Lett. **103**, 155702 (2009).

[20] W. Hu, S. Kaiser, D. Nicoletti, C. R. Hunt, I. Gierz, M. C. Hoffmann, M. Le Tacon, T. Loew, B. Keimer, and A. Cavalleri, Optically enhanced coherent transport in $YBa_2Cu_3O_{6.5}$ by ultrafast redistribution of interlayer coupling, Nat. Mater. **13**, 705 (2014).

[21] R. Mankowsky, A. Subedi, M. Först, S. O. Mariager, M. Chollet, H. T. Lemke, J. S. Robinson, J. M. Glownia, M. P. Minitti, A. Frano, M. Fechner, N. A. Spaldin, T. Loew, B. Keimer, A. Georges, and A. Cavalleri, Nonlinear lattice dynamics as a basis for enhanced superconductivity in $YBa_2Cu_3O_{6.5}$, Nature (London) **516**, 71 (2014).

[22] S. Kaiser, C. R. Hunt, D. Nicoletti, W. Hu, I. Gierz, H. Y. Liu, M. Le Tacon, T. Loew, D. Haug, B. Keimer, and A. Cavalleri, Optically enhanced coherent transport far above t_c in underdoped $YBa_2Cu_3O_{6.5}$, Phys. Rev. B **89**, 184516 (2014).

[23] N. H. Lindner, G. Refael, and V. Galitski, Floquet topological insulator in semiconductor quantum wells, Nat. Phys. **7**, 490 (2011).

[24] M. Sato, S. Takayoshi, and T. Oka, Laser-Driven Multiferroics and Ultrafast Spin Current Generation, Phys. Rev. Lett. **117**, 147202 (2016).

[25] D. Ceresoli and E. Tosatti, Berry-Phase Calculation of Magnetic Screening and Rotational g Factor in Molecules and Solids, Phys. Rev. Lett. **89**, 116402 (2002).

[26] D. Ceresoli, Berry phase calculations of the rotational and pseudorotational g-factor in molecules and solids, Ph.D. thesis, Scuola Internazionale Superiore di Studi Avanzati (SISSA), Trieste, 2002, available online at http://citeseerx.ist.psu.edu/viewdoc/download?doi=10.1.1.439.9823&rep=rep1&type=pdf.

[27] A. Einstein and W. J. de Haas, Experimental proof of the existence of Ampère's molecular currents, Proc. KNAW **18**, 696 (1915).

[28] G. C. Wick, On the magnetic field of a rotating molecule, Phys. Rev. **73**, 51 (1948).

[29] J. R. Eshbach and M. W. P. Strandberg, Rotational magnetic moments of $^1\Sigma$ molecules, Phys. Rev. **85**, 24 (1952).

[30] W. Hüttner, H. K. Bodenseh, and P. Nowicki, The vibrational Zeeman effect in HC ≡ CF and DC ≡ CF, Mol. Phys. **35**, 729 (1978).

[31] R. E. Moss and A. J. Perry, The vibrational Zeeman effect, Mol. Phys. **25**, 1121 (1973).

[32] E. Anastassakis, E. Burstein, A. A. Maradudin, and R. Minnick, Morphic effects. III. Effects of an external magnetic field on the long wavelength optical phonons, J. Phys. Chem. Solids **33**, 519 (1972).

[33] Y. T. Rebane, Faraday effect produced in the residual ray region by the magnetic moment of an optical phonon in an ionic crystal, Zh. Eksp. Teor. Fiz. **84**, 2323 (1983) [Sov. Phys. JETP **57**, 1356 (1983)].

[34] P. S. Riseborough, Quantum fluctuations in insulating ferroelectrics, Chem. Phys. **375**, 184 (2010).

[35] I. E. Dzyaloshinskii and E. I. Kats, Sound waves in solids in magnetic field, Europhys. Lett. **96**, 46001 (2011).

[36] N. Koshizuka and S. Ushioda, Inelastic-light-scattering study of magnon softening in $ErFeO_3$, Phys. Rev. B **22**, 5394 (1980).

[37] D. M. Juraschek, M. Fechner, and N. A. Spaldin, Ultrafast Structure Switching through Nonlinear Phononics, Phys. Rev. Lett. **118**, 054101 (2017).

[38] G. Kresse and J. Furthmüller, Efficiency of *ab initio* total energy calculations for metals and semiconductors using a plane-wave basis set, Comput. Mater. Sci. **6**, 15 (1996).

[39] G. Kresse and J. Furthmüller, Efficient iterative schemes for *ab initio* total-energy calculations using a plane-wave basis set, Phys. Rev. B **54**, 11169 (1996).

[40] A. Togo and I. Tanaka, First-principles phonon calculations in materials science, Scr. Mater. **108**, 1 (2015).

[41] G. I. Csonka, J. P. Perdew, A. Ruzsinszky, P. H. T. Philipsen, S. Lebègue, J. Paier, O. A. Vydrov, and J. G. Ángyán, Assessing the performance of recent density functionals for bulk solids, Phys. Rev. B **79**, 155107 (2009).

[42] M. Eibschütz, Lattice constants of orthoferrites, Acta Crystallogr. **19**, 337 (1965).

[43] J. M. Kiat and T. Roisnel, Rietveld analysis of strontium titanate in the Müller state, J. Phys.: Condens. Matter **8**, 3471 (1996).

[44] P. A. Fleury, J. F. Scott, and J. M. Worlock, Soft Phonon Modes and the 110 °K Phase Transition in $SrTiO_3$, Phys. Rev. Lett. **21**, 16 (1968).

[45] J. C. Galzerani and R. S. Katiyar, The infrared reflectivity in $SrTiO_3$ and the antidistortive transition, Solid State Commun. **41**, 515 (1982).

[46] G. V. Subba Rao, C. N. R. Rao, and J. R. Ferraro, Infrared and electronic spectra of rare earth perovskites: Ortho-chromites, -manganites, and -ferrites, Appl. Spectrosc. **24**, 436 (1970).

[47] A. Pimenov, A. A. Mukhin, V. Yu. Ivanov, V. D. Travkin, A. M. Balbashov, and A. Loidl, Possible evidence for electromagnons in multiferroic manganites, Nat. Phys. **2**, 97 (2006).

[48] D. Senff, P. Link, K. Hradil, A. Hiess, L. P. Regnault, Y. Sidis, N. Aliouane, D. N. Argyriou, and M. Braden, Magnetic Excitations in Multiferroic $TbMnO_3$: Evidence for a Hybridized Soft Mode, Phys. Rev. Lett. **98**, 137206 (2007).

[49] A. B. Sushkov, M. Mostovoy, R. Valdés Aguilar, S.-W. Cheong, and H. D. Drew, Electromagnons in multiferroic RMn_2O_5 compounds and their microscopic origin, J. Phys.: Condens. Matter **20**, 434210 (2008).

[50] N. Kida, Y. Ikebe, Y. Takahashi, J. P. He, Y. Kaneko, Y. Yamasaki, R. Shimano, T. Arima, N. Nagaosa, and Y. Tokura, Electrically driven spin excitation in the ferroelectric magnet $DyMnO_3$, Phys. Rev. B **78**, 104414 (2008).

[51] R. V. Aguilar, M. Mostovoy, A. B. Sushkov, C. L. Zhang, Y. J. Choi, S. W. Cheong, and H. D. Drew, Origin of Electromagnon Excitations in Multiferroic $R\mathrm{MnO}_3$, Phys. Rev. Lett. **102**, 047203 (2009).

[52] A. Pimenov, A. Shuvaev, A. Loidl, F. Schrettle, A. A. Mukhin, V. D. Travkin, V. Yu. Ivanov, and A. M. Balbashov, Magnetic and Magnetoelectric Excitations in $TbMnO_3$, Phys. Rev. Lett. **102**, 107203 (2009).

[53] J. S. Lee, N. Kida, S. Miyahara, Y. Takahashi, Y. Yamasaki, R. Shimano, N. Furukawa, and Y. Tokura, Systematics of electromagnons in the spiral spin-ordered states of $R\mathrm{MnO}_3$, Phys. Rev. B **79**, 180403(R) (2009).

[54] Y. Takahashi, R. Shimano, Y. Kaneko, H. Murakawa, and Y. Tokura, Magnetoelectric resonance with electromagnons in a perovskite helimagnet, Nat. Phys. **8**, 121 (2012).

[55] H. Katsura, A. V. Balatsky, and N. Nagaosa, Dynamical Magnetoelectric Coupling in Helical Magnets, Phys. Rev. Lett. **98**, 027203 (2007).

[56] A. Pimenov, A. M. Shuvaev, A. A. Mukhin, and A. Loidl, Electromagnons in multiferroic manganites, J. Phys.: Condens. Matter **20**, 434209 (2008).

[57] A. M. Shuvaev, V. D. Travkin, V. Yu. Ivanov, A. A. Mukhin, and A. Pimenov, Evidence for Electroactive Excitation of the Spin Cycloid in $TbMnO_3$, Phys. Rev. Lett. **104**, 097202 (2010).

[58] Y. Takahashi, Y. Yamasaki, and Y. Tokura, Terahertz Magnetoelectric Resonance Enhanced by Mutual Coupling of Electromagnons, Phys. Rev. Lett. **111**, 037204 (2013).

[59] A. Shuvaev, V. Dziom, A. Pimenov, M. Schiebl, A. A. Mukhin, A. C. Komarek, T. Finger, M. Braden, and A. Pimenov, Electric Field Control of Terahertz Polarization in a Multiferroic Manganite with Electromagnons, Phys. Rev. Lett. **111**, 227201 (2013).

[60] M. Mochizuki and N. Furukawa, Microscopic model and phase diagrams of the multiferroic perovskite manganites, Phys. Rev. B **80**, 134416 (2009).

[61] M. Mochizuki, N. Furukawa, and N. Nagaosa, Spin Model of Magnetostrictions in Multiferroic Mn Perovskites, Phys. Rev. Lett. **105**, 037205 (2010).

[62] L. P. Pitaevskiĭ, Electric forces in a transparent dispersive medium, J. Exptl. Theoret. Phys. (U.S.S.R.) **39**, 1450 (1960) [Sov. Phys. JETP **12**, 1008 (1961)].

[63] J. P. van der Ziel, P. S. Pershan, and L. D. Malmstrom, Optically-Induced Magnetization Resulting from the Inverse Faraday Effect, Phys. Rev. Lett. **15**, 190 (1965).

[64] P. S. Pershan, J. P. van der Ziel, and L. D. Malmstrom, Theoretical discussion of the inverse Faraday effect, Raman scattering, and related phenomena, Phys. Rev. **143**, 574 (1966).

[65] A. V. Kimel, A. Kirilyuk, P. A. Usachev, R. V. Pisarev, A. M. Balbashov, and T. Rasing, Ultrafast non-thermal control of magnetization by instantaneous photomagnetic pulses, Nature (London) **435**, 655 (2005).

[66] M. Battiato, G. Barbalinardo, and P. M. Oppeneer, Quantum theory of the inverse Faraday effect, Phys. Rev. B **89**, 014413 (2014).

[67] A. H. M. Reid, A. V. Kimel, A. Kirilyuk, J. F. Gregg, and T. Rasing, Investigation of the femtosecond inverse Faraday effect using paramagnetic $Dy_3Al_5O_{12}$, Phys. Rev. B **81**, 104404 (2010).

[68] D. Popova, A. Bringer, and S. Blügel, Theory of the inverse Faraday effect in view of ultrafast magnetization experiments, Phys. Rev. B **84**, 214421 (2011).

[69] S. Ali, J. R. Davies, and J. T. Mendonca, Inverse Faraday Effect with Linearly Polarized Laser Pulses, Phys. Rev. Lett. **105**, 035001 (2010).

[70] M. Matsubara, S. Manz, M. Mochizuki, T. Kubacka, A. Iyama, N. Aliouane, T. Kimura, S. L. Johnson, D. Meier, and M. Fiebig, Magnetoelectric domain control in multiferroic $TbMnO_3$, Science **348**, 1112 (2015).

[71] L. Zhang and Q. Niu, Angular Momentum of Phonons and the Einstein–de Haas Effect, Phys. Rev. Lett. **112**, 085503 (2014).

[72] D. Liu and J. Shi, Circular phonon dichroism in Weyl semimetals, arXiv:1609.07282.

[73] P. Rovillain, M. Cazayous, Y. Gallais, M. A. Measson, A. Sacuto, H. Sakata, and M. Mochizuki, Magnetic Field Induced Dehybridization of the Electromagnons in Multiferroic $TbMnO_3$, Phys. Rev. Lett. **107**, 027202 (2011).

[74] G. Schaack, Magnetic-field dependent phonon states in paramagnetic CeF_3, Solid State Commun. **17**, 505 (1975).

[75] G. Schaack, Observation of circularly polarized phonon states in an external magnetic field, J. Phys. C: Solid State Phys. **9**, L297 (1976).

[76] G. Schaack, Magnetic field dependent splitting of doubly degenerate phonon states in anhydrous cerium-trichloride, Z. Phys. B **26**, 49 (1977).

[77] S. Rémi, B. B. Goldberg, and A. K. Swan, Charge Tuning of Nonresonant Magnetoexciton Phonon Interactions in Graphene, Phys. Rev. Lett. **112**, 056803 (2014).

[78] C. Strohm, G. L. J. A. Rikken, and P. Wyder, Phenomenological Evidence for the Phonon Hall Effect, Phys. Rev. Lett. **95**, 155901 (2005).

[79] L. Sheng, D. N. Sheng, and C. S. Ting, Theory of the Phonon Hall Effect in Paramagnetic Dielectrics, Phys. Rev. Lett. **96**, 155901 (2006).